DOI: 10.61782/fa.2025.0383

FORUM ACUSTICUM EURONOISE 2025

EXPLORATION OF USE OF MEMBRANE-TYPE METAMATERIAL LAYER FOR APPLICATION IN BUILDING ACOUSTICS

Rui ZENG[1,2,3*] **Elke DECKERS**[1,4] **Christ GLORIEUX**[5]
Daniel URBAN[2,6] **Bartosz CHMIELEWSKI**[3]
[1] Department of Mechanical Engineering, KU Leuven, Belgium
[2] Department of Materials Engineering and Physics, STU Bratislava, Slovakia
[3] KFB Acoustics Sp. z o. o., Oławska 8, 55-040 Domasław, Poland
[4] Flanders Make @ KU Leuven, Diepenbeek, Belgium
[5] Department of Physics and Astronomy, KU Leuven, Belgium
[6] Faculty of Civil end Environmental Engineering, TU Wien, Austria

ABSTRACT

This study investigates the sound transmission loss (STL) and absorption performance of a membrane-type metamaterial layer through a series of controlled experiments. Measurements were conducted in an impedance tube to independently characterize the STL and absorption properties of the metamaterial layer. Based on the results from numerical simulations and impedance tube measurements, a larger-scale prototype layer was designed and tested in a transmission room configuration, for verifying the potential for application as part of acoustic insulation solutions in retrofitting applications.

Keywords: *membrane-type acoustic metamaterials, sound transmission loss, architectural acoustics, impedance tube measurement, transmission chamber test*

1. INTRODUCTION

Low-frequency noise insulation presents a significant challenge in building acoustics, particularly in lightweight structures where traditional solutions often fall short in performance. Due to its long wavelength, low-frequency sound can efficiently propagate through walls, making it difficult to attenuate using conventional porous absorbers. Increasing mass is an effective way to improve sound insulation, but in many applications, especially in retrofitting, adding substantial weight is neither practical nor desirable.

In retrofitting applications, where modifications to existing structures are constrained by space, weight, and cost, improving low-frequency sound insulation is particularly challenging. Common strategies involve adding additional panels, integrating resilient layers for decoupling, or incorporating insulation boards. While these approaches can enhance sound insulation in certain frequency ranges, they may also introduce resonance effects that degrade performance in others [1].

Acoustic metamaterials have been explored as a complementary solution to conventional sound insulation approaches by utilizing locally resonant mechanisms to enhance STL in targeted frequency bands [2–5]. Among them, membrane-type metamaterials have attracted increasing attention due to their ability to achieve strong low-frequency sound insulation with limited added mass. These metamaterials typically consist of a tensioned membrane with an attached mass, forming a resonant system that blocks sound transmission at specific frequencies [6]. Despite extensive studies on the fundamental properties of membrane-type metamaterials, their large-scale application in building acoustics remains unexplored. Most existing research has focused on numerical modeling and small-scale impedance tube measurements, with limited investigations into their performance

**Corresponding author*: *rui.zeng@kfb-acoustics.com.*

in configurations relevant to architectural acoustics.

This study investigates the sound transmission loss and absorption performance of a membrane-type metamaterial layer through a series of controlled experiments. The primary objectives are:

- To evaluate the STL and absorption properties of the metamaterial layer through impedance tube experiments.
- To compare numerical simulations with experimental results.
- To assess the effectiveness of a scaled-up prototype for practical building applications.

These studies lay the groundwork for future research and fine-tuning of metamaterial designs for practical applications.

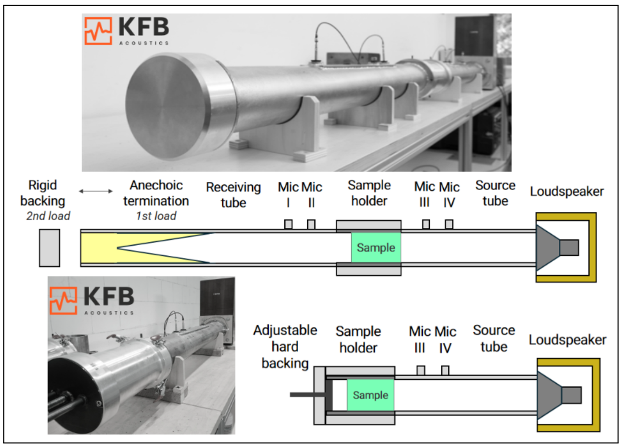

Figure 1. Impedance tube set-up for sound transmission loss and absorption measurements.

2. EXPERIMENTAL AND NUMERICAL METHODS

2.1 Membrane Material

A commercially available black rubber sheet with a nominal thickness of $1\,\mathrm{mm}$ was used for the membrane, selected for its accessibility rather than specific mechanical properties, as detailed parameter measurements were not available. The density of the rubber was estimated through simple mass and volume measurements, yielding a value of $1590\,\mathrm{kg\,m^{-3}}$ with an uncertainty of $40\,\mathrm{kg\,m^{-3}}$.

2.2 Impedance Tube Measurements

The impedance tube (see Fig. 1), custom-made by KFB Acoustics for studying this case, has an internal acoustic passage diameter $102\,\mathrm{mm}$. A sample holder with steel rings was designed to clamp the membrane, with the membrane's outer diameter being $122.5\,\mathrm{mm}$.

The membrane samples for the impedance tube, as shown in Fig. 2, were manually cut and bonded to two steel rings on each side for structural support, ensuring a fixed boundary condition for the impedance tube experiments. The edges of the ring-rubber-ring sample were polished smooth, and slight unevenness was introduced during manual fabrication. The pretension in the membrane was assumed to be small, as the manual stretching process aimed only at flattening the membrane without inducing significant pre-stress. Additionally, modified samples were prepared by attaching one or two identical cylindrical steel masses ($1.85\,\mathrm{g}$ each, $10\,\mathrm{mm}$ diameter, $3\,\mathrm{mm}$

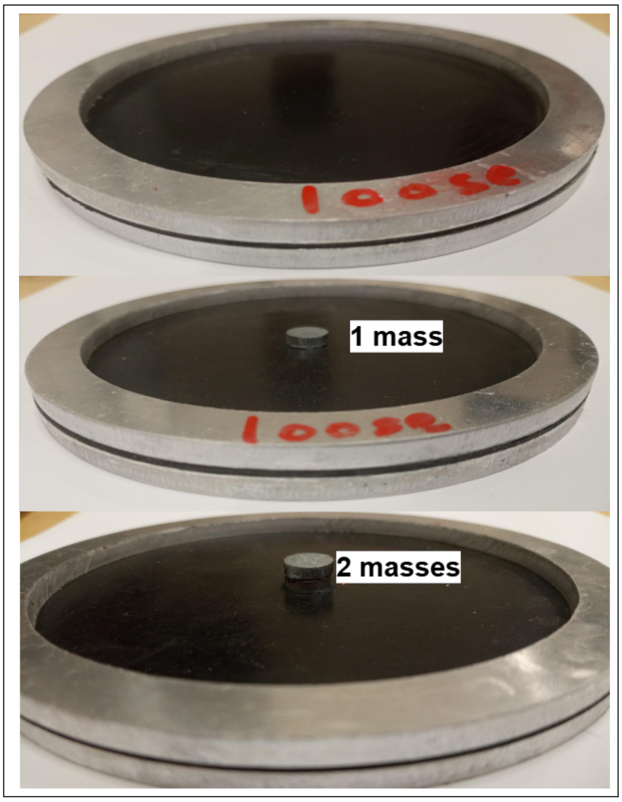

Figure 2. Membrane samples using the same $1\,\mathrm{mm}$ rubber: (1) plain membrane, (2) with one central mass ($10\,\mathrm{mm}$ diameter, $3\,\mathrm{mm}$ thick), (3) with two stacked masses (total $6\,\mathrm{mm}$). Edges clamped with steel rings.

thickness) at the membrane center. Two such masses were stacked in the two-mass configuration, resulting in a total thickness of 6 mm.

The test frequency range spanned from 50 Hz to 1600 Hz. White noise was used as the excitation source, with its level carefully adjusted to avoid nonlinear effects and prevent structural vibrations of the tube or mounting components. Each experiment was repeated three times for the sake of checking consistency.

For the STL measurements, a four-microphone configuration was employed, with an anechoic termination to minimize reflections, following ASTM E2611 [7]. Absorption measurements utilized a two-microphone setup with a rigid backing, in accordance with ISO 10534 [8]. The rigid backing distance from the sample was adjustable to explore different resonance conditions by varying the air gap between the membrane and the backing. In this study, two air gap configurations were tested, with the rigid backing positioned to create an 50 mm air gap and an 100 mm air gap.

Prior to testing, a reference measurement was conducted with an empty tube. The results confirmed that the presence of the steel rings did not introduce significant effects on measurements within the selected frequency range.

2.3 Impedance Tube Simulation

Numerical simulations were conducted using the finite element method (FEM) in COMSOL Multiphysics [9] to analyze the sound transmission loss and absorption performance of the membrane-type resonator. The simulation follows the impedance tube approach in [10] with modified material parameters and implementation. Specifically, incident wave excitation and non-reflecting boundaries were replaced by port-based plane wave excitation and termination, ensuring accurate sound power calculations. Additionally, the membrane was modeled with the Shell Module to capture its flexural motion. The tube was assumed to be rigid, and the membrane edges were set to fixed, consistent with the experimental setup.

Two simulation configurations, as illustrated in Fig. 3, were implemented to correspond with the experimental setups:

- Sound Transmission Loss Simulation: The impedance tube was modeled as a cylindrical waveguide with an internal diameter of 102 mm, matching the actual acoustic passage in the experiment. The STL was obtained by calculating the ratio of incident to transmitted acoustic power at the respective ports.
- Absorption Simulation: A rigid backing was introduced at a controlled distance behind the membrane to investigate absorption characteristics. The absorption coefficient was determined by subtracting the ratio of reflected to incident acoustic power from one at the input port.

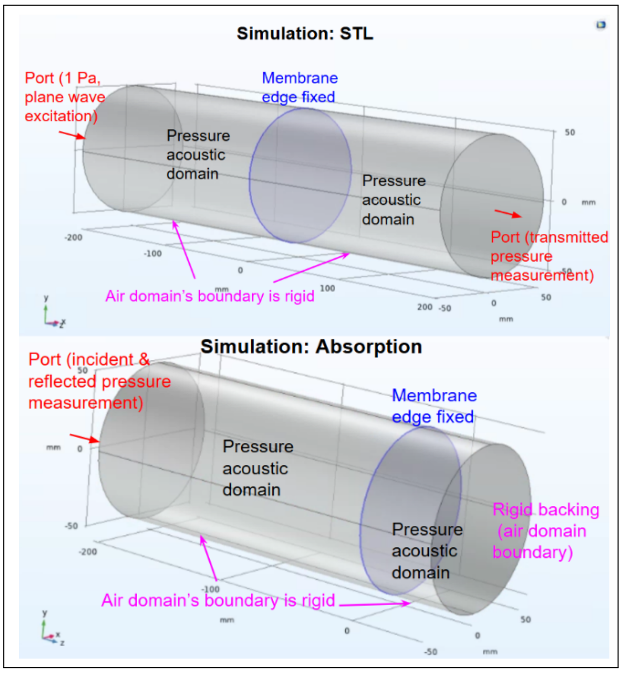

Figure 3. Schematic of the simulation setup of the impedance tube.

The computational domain was discretized using free tetrahedral elements with normal resolution, following built-in mesh size calibration for general physics applications. The number of degrees of freedom in the simulation ranged from approximately 2977 to 3033, depending on the configuration.

Since the exact viscoelastic properties of the rubber membrane were unknown, the material parameters in the simulation were taken from [11], which measured a similar type of rubber. However, these measured values have significant uncertainties, meaning the chosen parameters are only rough estimates. As a result, any differences between the simulation and experiment may be partly due to inaccuracies in the material properties.

2.4 Transmission Chamber Test

The transmission loss measurements were conducted in the V1 Laboratory test stand at the Acoustic Research and Innovation Centre (KFB Acoustics, Poland), designed for measuring airborne sound insulation of vertical partitions and components according to ISO 10140 with standardized window openings. The experimental facility is shown in Fig. 4.

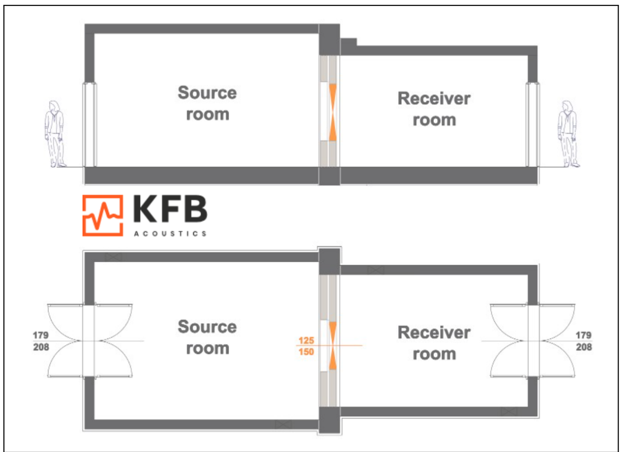

Figure 4. Experimental facility for the transmission chamber test.

Seven configurations were examined:
(1) Steel: a 1.5 mm thick steel plate
(2) Rubber: a 1 mm thick rubber layer
(3) Rubber–Air Gap–Steel: a 1 mm rubber layer with a 50 mm air gap and a steel plate
(4) Membrane Metamaterial: a 1 mm rubber layer supported by a perforated 1.5 mm steel frame with circular cutouts (102 mm diameter, 30 mm spacing)
(5) Membrane Metamaterial–Air Gap–Steel: the metamaterial with a 50 mm air gap and steel plate
(6) Metamaterial + Mass: the metamaterial with a central steel mass in each unit cell
(7) Metamaterial + Mass–Air Gap–Steel: the metamaterial with masses, plus a 50 mm air gap and steel plate.

All samples were mounted in a wooden frame to maintain consistent boundary conditions. As shown in Fig. 5, configuration (6)—a metamaterial with central masses—serves as a representative example of the tested samples, which were assembled within a standardized test window (1250 mm × 1500 mm).

Measurements were conducted following standardized procedures to evaluate the STL of large-scale samples. Two measurement approaches were employed to ensure both standardized evaluation and high-resolution analysis:

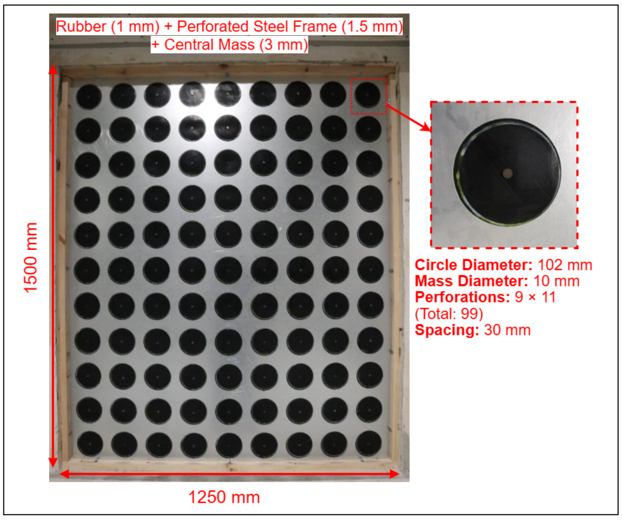

Figure 5. Configuration (6): membrane-type metamaterial consisting of a 1 mm-thick rubber layer and a perforated 1.5 mm-thick steel frame (9 × 11 circular cutouts, 102 mm diameter, 30 mm spacing), with a central steel mass (10 mm diameter, 3 mm thick) in each unit cell.

- Method 1 (ISO 10140 [12]): A calibrated omnidirectional loudspeaker generated white noise. Reverberation time (RT60) as measured via the interrupted noise method at six microphone positions. The STL measurements were performed using the Norsonic Nor850 Measurement System with a rotating boom for spatial averaging. Additionally, microphone signals were split: one for 1/3-octave band processing, the other recorded for finer-resolution post-processing.
- Method 2 (ISO 18233 [13]): A custom logarithmic sine sweep (40 Hz–2000 Hz, 10 s duration + 5 s silence) was used as excitation, played from the same loudspeaker. The signal was played and recorded using the Head Acoustic SQuadriga III module. Measurements were conducted with fixed loudspeaker and microphone positions to maintain time-invariance. The STL was computed based on the difference in impulse responses measured in the source and receiving rooms, while RT60 was de-

rived using the Schroeder integral method. This method enables post-processing in both 1/3-octave bands and finer resolution (every 5 Hz).

3. RESULTS AND DISCUSSION

3.1 STL and Absorption in Impedance Tube

Impedance tube measurements for STL and absorption (Fig. 6, Fig. 7) provide insights into membrane acoustic performance.

As observed in Fig. 6, even the plain rubber sample exhibits a notable STL peak around 200 Hz, reaching approximately 14 dB. This peak can be attributed to the lowest vibrational mode induced by the fixed boundary conditions at the sample's edges. Apart from its resonance, the overall STL trend increases with frequency, which aligns with the expected mass-law trend of a single material layer.

Introducing a small steel mass at the membrane center modifies the vibrational response, leading to a shift of the main STL peak toward lower frequencies. The STL magnitude at resonance is also enhanced, indicating improved low-frequency isolation. Using two masses amplifies this effect, showing that localized mass can tune the membrane's resonance behavior, as also reported in literature [14].

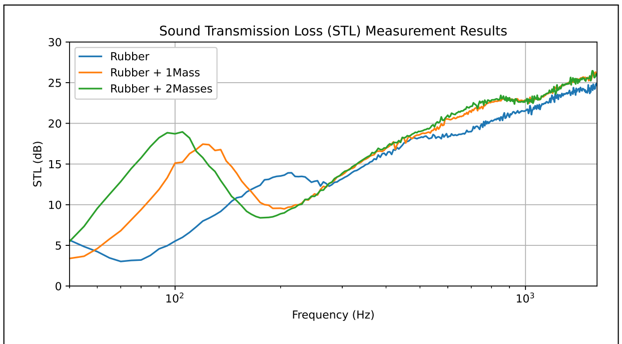

Figure 6. Impedance tube measurement for sound transmission loss of three rubber samples.

The absorption coefficients of the samples, measured under different air gap configurations (50 mm and 100 mm), are presented in Fig. 7. The plain rubber membrane exhibits multiple absorption peaks, with the first low-frequency peak becoming more pronounced and shifting to lower frequencies as the air gap increases, suggesting a significant membrane-cavity interaction, with the membrane as mass and the air cavity as a spring. The second peak corresponds to the membrane's structural mode, which is less affected by the air gap.

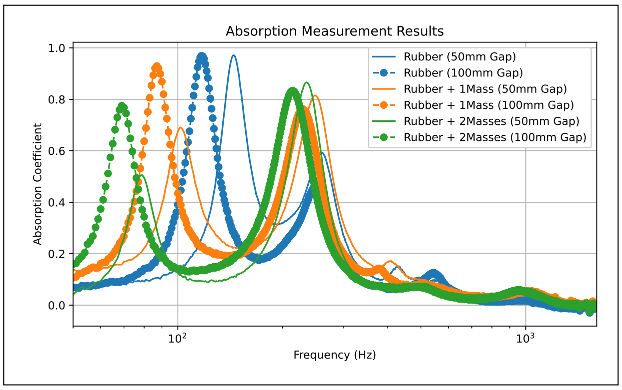

Figure 7. Impedance tube measurement for absorption of three rubber samples under different air gap configurations.

When a single steel mass is added, the first absorption peaks move to lower frequencies, similar to the trend seen in the STL results. This suggests that the added mass changes the membrane's resonance, affecting how it interacts with the backing cavity. With two masses, the resonance shifts further to lower frequencies, although the absorption amplitude becomes smaller.

To further validate the impedance tube results, another rubber sample without added mass was tested, and its STL and absorption performance were compared with simulations, as shown in Fig. 8 and Fig. 9. Due to the differences in experimental setups—STL measured for the membrane alone and absorption measured with a 50 mm air gap and a rigid backing—the two cannot be directly compared. However, both experimental and simulated results revealed a complementary relationship between STL and absorption.

In the STL results, the simulation captures the first and second resonance peaks observed experimentally, while the absorption simulation identifies three primary peaks, aligning well with the measurements. The main STL peak and absorption peaks appear in similar frequency regions, confirming that the numerical model accurately represents the essential resonance behavior of the membrane.

This complementary relationship is reflected in the resonance characteristics: STL peaks correspond to absorption dips, as strong resonance blocks sound transmis-

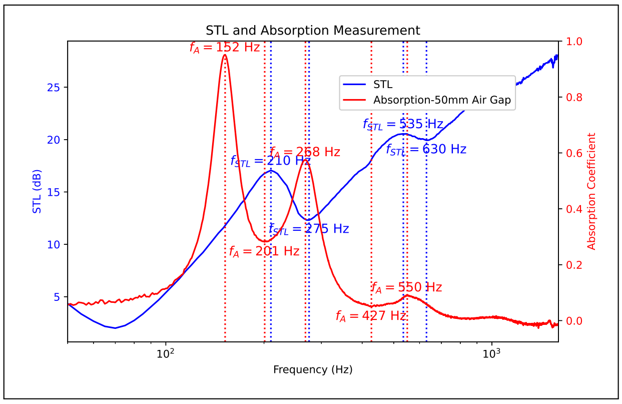

Figure 8. Measured sound transmission loss (STL) and absorption coefficient of a rubber sample without added mass. Peaks and dips are marked to indicate resonance behaviors.

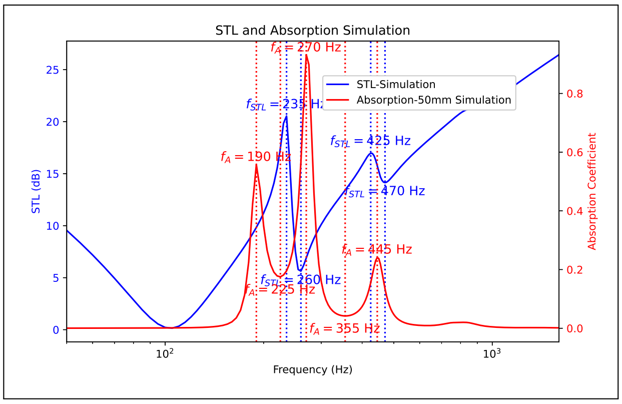

Figure 9. Simulated STL and absorption coefficient of a rubber sample without added mass. Marked peaks and dips highlight resonance effects captured in the model.

sion but increases reflection, reducing energy dissipation. Conversely, absorption peaks occur when the membrane couples more effectively with the backing cavity, enhancing energy dissipation and reducing STL. However, in the STL experiment, the membrane vibrates without the rigid backing, so while STL and absorption show a complementary trend, their peaks and dips don't always align.

It is further important to recognize that the precise values of STL and absorption in the simulation are highly dependent on the assumed material parameters. Factors such as mass per unit area, elastic properties, pre-stress conditions, and damping characteristics can all impact the frequency and amplitude of the response. Though not detailed here, these factors are relevant for future model refinement.

3.2 STL Results in the Transmission Chamber

Figures 10 and 11 show STL measurements in 1/3-octave bands from the transmission chamber, obtained using the Norsonic analyzer for both single-layer and double-layer configurations, with the single value Rw included.

In the single-layer case (Figure 10), the steel panel shows the highest STL across the full frequency range, following the expected mass law behavior. In contrast, the much lighter rubber panel exhibits significantly lower STL. A dip around 80 Hz for both steel and rubber may result from the coupling of the room and sample. It should be noted that results below 100 Hz are presented for informational purposes only, as they fall outside the effective measurement range of the laboratory setup, where uncertainties in the data may arise. The membrane metamaterial (rubber bonded to a perforated steel frame) improves the STL over plain rubber, performing better above 160 Hz. The dip observed around 80 Hz for steel and rubber appears shifted in the metamaterial, likely due to changes in resonance behavior. Adding a central mass to the membrane further enhances the STL below 200 Hz, indicating a local resonance mechanism.

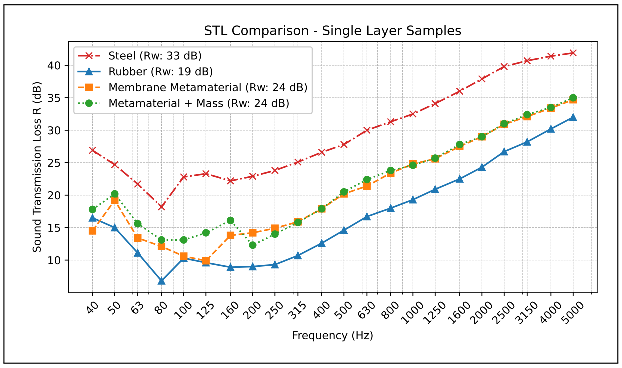

Figure 10. STL of single-layer samples measured using the Norsonic analyzer.

The double-layer samples (Figure 11) represent a more realistic wall structure, consisting of a decoupled cavity between a front rubber layer and a steel panel. Compared to single-layer configurations, the rubber–air–steel structure already achieves higher STL in the

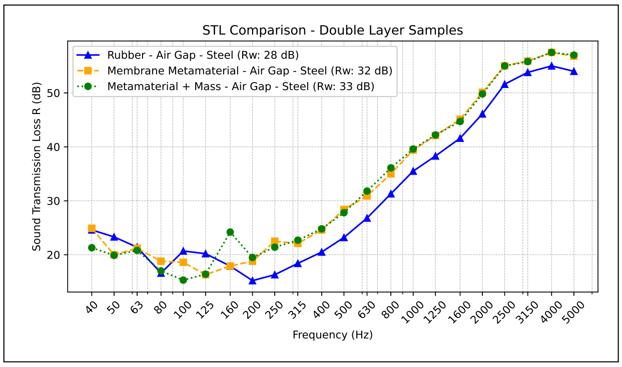

Figure 11. STL of double-layer samples measured using the Norsonic analyzer.

mid-to-high frequency range due to added mass and decoupling. However, a low-frequency dip appears around 200 Hz, resulting from the mass-spring-mass resonance, within the range predicted by a typical resonance calculation (e.g., [[1]]).

Replacing the rubber layer with a membrane metamaterial, the 200 Hz dip of the rubber–air–steel configuration becomes less noticeable. The overall STL improves in the mid-to-high frequency range, due to increased surface density. More significantly, the metamaterial introduces an STL enhancement around 250 Hz, attributed to local resonance effects. Adding a central mass shifts the resonance to around 160 Hz, improving the STL by about 6 dB compared to the rubber–air–steel configuration at this frequency.

The low-frequency STL enhancement observed in the transmission chamber is consistent with impedance tube measurements. In both setups, adding a central mass shifts the dominant resonance toward lower frequencies and increases STL, though the resonance peaks appear at different frequencies due to boundary conditions and interactions with the surrounding frame and air cavity.

This confirms that locally resonant metamaterials can improve sound insulation in both idealized tube and realistic large-scale wall applications.

To complement the standardized ISO 10140 measurements, two alternative methods—noise recording and swept-sine signal excitation—were used to extract the level difference between the source and receiver rooms at finer frequency resolution. The level difference improvement, shown in 1/3-octave bands (Figure 12) and at finer frequency resolution (Figure 13), quantifies the increased isolation achieved by the metamaterial samples compared to the rubber reference.

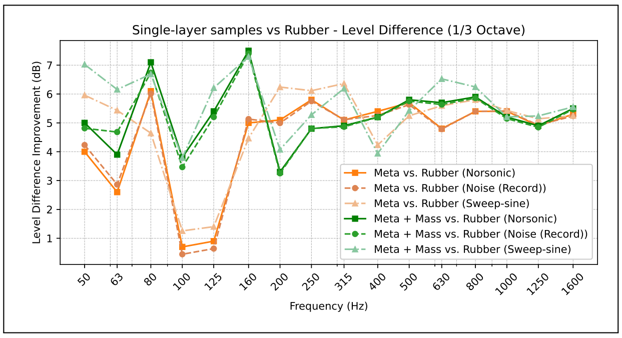

Figure 12. Effect of single-layer metamaterial samples on sound pressure level difference between source and receiving rooms, compared to the rubber reference, in 1/3-octave bands using three methods.

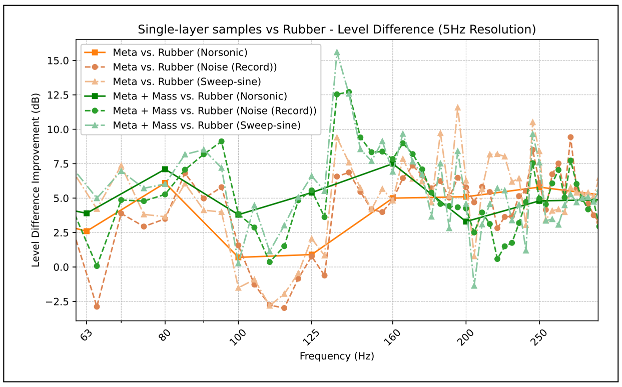

Figure 13. Level difference improvement (60–300 Hz) of single-layer metamaterials over rubber, 5 Hz resolution.

In 1/3-octave bands, all methods show similar trends. The noise recording data aligns well with Norsonic data, while swept-sine shows greater deviation. At finer resolution (5 Hz), swept-sine reveals sharper low-frequency peaks, suggesting better sensitivity to local resonance, although small mismatches due to timing, filtering, or noise remain.

Given the current stage of development, the ISO 10140 method provides the most stable and interpretable data for comparison across configurations and is therefore used as the primary dataset in this study.

4. CONCLUSION

This study investigated the sound insulation performance of a membrane-type acoustic metamaterial layer through a combination of numerical simulations, impedance tube measurements, and scaled-up transmission chamber tests. The results confirm the presence of low-frequency STL enhancement due to local resonance effects, particularly when central masses are added to the membrane. These effects were consistently observed across both small and large experimental configurations, demonstrating the metamaterial's potential for application in lightweight and retrofittable wall systems.

Despite the promising results, several limitations remain. Variations in sample fabrication, limited control over membrane pretension, and measurement uncertainties—especially in fine-resolution methods—may affect the accuracy of the results. Additionally, material parameter uncertainties in simulations restrict direct quantitative comparisons.

Future work will focus on improving sample consistency, refining structural designs to better control resonance frequencies, and implementing higher-precision measurement workflows. These developments aim to further explore and optimize the practical application of membrane-type metamaterials in building acoustics.

5. ACKNOWLEDGMENTS

This project has received funding from the European Union's Horizon Europe research & innovation programme under the HORIZON-MSCA-2021-DN-01 grant agreement No. 101072598 –"ActaReBuild".

6. REFERENCES

[1] R. Zeng, E. Deckers, C. Glorieux, D. Urbán, and B. Chmielewski, "Wall-applicable metamaterial: mitigating resonance dip for enhanced sound transmission loss," in *Proc. INTER-NOISE and NOISE-CON*, pp. 7144–7155, 2024.

[2] N. B. Roozen, D. Urban, E. A. Piana, and C. Glorieux, "On the use of dynamic vibration absorbers to counteract the loss of sound insulation due to mass-spring-mass resonance effects in external thermal insulation composite systems," *Applied Acoustics*, vol. 178, p. 107999, 2021.

[3] G. Ji and J. Huber, "Recent progress in acoustic metamaterials and active piezoelectric acoustic metamaterials: a review," *Appl. Mater. Today*, vol. 26, p. 101260, 2022.

[4] Y. Zhang, J. Zhang, Y. Li, D. Yao, Y. Zhao, Y. Ai, W. Pan, and J. Li, "Research progress on thin-walled sound insulation metamaterial structures," in *Acoustics*, vol. 6, pp. 298–330, 2024.

[5] A. Arjunan, A. Baroutaji, J. Robinson, A. Vance, and A. Arafat, "Acoustic metamaterials for sound absorption and insulation in buildings," *Build. Environ.*, p. 111250, 2024.

[6] C. Wang, L. Cai, M. Gao, L. Jin, L. Sun, X. Tang, G. Shi, X. Zheng, and C. Guo, "Manufacturing of membrane acoustical metamaterials for low frequency noise reduction and control: a review," *Mech. Adv. Mater. Struct.*, vol. 31, no. 25, pp. 7008–7023, 2024.

[7] "Standard test method for measurement of normal incidence sound transmission of acoustical materials based on the transfer matrix method," Tech. Rep. ASTM E2611-19, ASTM International, 2019.

[8] "Acoustics — determination of sound absorption coefficient and impedance in impedance tubes — part 2: Transfer-function method," Tech. Rep. ISO 10534-2, International Organization for Standardization, 1998.

[9] COMSOL AB, *COMSOL Multiphysics® v. 6.1*, 2022.

[10] R. Zeng, E. Deckers, C. Glorieux, D. Urbán, and B. Chmielewski, "Locally resonant metamaterial wall targeting tonal noise arising from heat pumps in residential buildings," in *Proc. ISMA 2024—Int. Conf. on Noise and Vibration Eng.*, pp. 2652–2661, 2024.

[11] A. Dobrucki, R. Bolejko, P. Nieradka, and A. Klimek, "Generalized oberst beam method for measuring viscoelastic parameters of layered composite components," *Arch. Mech.*, vol. 75, no. 1-2, pp. 27–52, 2023.

[12] "Acoustics — laboratory measurement of sound insulation of building elements," Tech. Rep. ISO 10140-2:2010, International Organization for Standardization, 2010.

[13] "Acoustics — application of new measurement methods in building and room acoustics," Tech. Rep. ISO 18233:2006, International Organization for Standardization, 2006.

[14] C. J. Naify, C.-M. Chang, G. McKnight, and S. Nutt, "Transmission loss and dynamic response of membrane-type locally resonant acoustic metamaterials," *J. Appl. Phys.*, vol. 108, no. 11, 2010.